



# Optimizing Thermal Efficiency and Emissions in Hybrid HCCI-DI Combustion with Biodiesel-Diethyl Ether-Nanoparticle Blends

G.M. Lionus LEO <sup>1,\*</sup>, S. SEKAR <sup>2</sup>, G. Ashwin PRABHU <sup>1</sup>, Prajith PRABHAKAR <sup>3</sup>

<sup>1</sup> Department of Mechanical Engineering, St. Joseph's College of Engineering, Chennai, Tamil Nadu, India.

<sup>2</sup> Department of Mechanical Engineering, Rajalakshmi Engineering College, Chennai, Tamil Nadu, India.

<sup>3</sup> Department of Mechanical Engineering, Saveetha School of Engineering, Saveetha Institute of Medical and Technical Sciences (SIMATS), Chennai, Tamil Nadu, India.

## ARTICLE INFO

2025, vol. 45, no.2, pp. 193-206

©2025 TIBTD Online.

doi: 10.47480/isibtcd.1630463

### Research Article

Received: 01 February 2025

Accepted: 27 March 2025

\* Corresponding Author

e-mail: lionusleo@gmail.com

### Keywords:

Neem oil biodiesel  
HCCI-DI combustion  
Nano additive  
Performance  
Emissions

### ORCID Numbers in author order:

0000-0002-8165-9901

0000-0000-0000-0000

0000-0001-5673-647X

0000-0002-5744-9365

## ABSTRACT

This study investigates the combustion, performance, and emissions of neem oil biodiesel blends in a Homogeneous Charge Compression Ignition-Direct Injection (HCCI-DI) engine, aiming to optimize engine efficiency and reduce environmental impact amid growing demands for sustainable alternatives to fossil fuels. The importance of this work lies in addressing the dual challenge of enhancing thermal efficiency while minimizing emissions through alternative fuels and advanced combustion strategies. Engine behaviour was analyzed based on biodiesel blending ratios (B25, B50, B75, B100), combustion modes (DI and HCCI-DI), and the addition of 50 ppm aluminum oxide ( $Al_2O_3$ ) nano-additives. Key findings show that increasing biodiesel content reduced peak in-cylinder pressures ( $P_{max}$ ) and heat release rates in both DI and HCCI-DI modes. Compared to DI, HCCI-DI improved combustion characteristics, with further enhancements from  $Al_2O_3$  nano-additives. Pure biodiesel (B100) decreased brake thermal efficiency (BTE) by 2.01% in DI and 1.68% in HCCI-DI relative to diesel. Still, HCCI-DI and nano-additives increased BTE for both diesel and biodiesel blends. Nitrogen oxide ( $NO_x$ ) emissions rose by 18.3% with B100 in DI mode but dropped by 4.3% in HCCI-DI with nano-additives. Hydrocarbon (HC) emissions fell by 52.17% with biodiesel in DI mode, though HCCI-DI increased them slightly; nano-additives reduced HC by up to 19.51%. Carbon monoxide (CO) emissions decreased by up to 55.56%, and smoke emissions dropped by 22.7% in DI and 39.1% in HCCI-DI with biodiesel, HCCI-DI, and nano-additives. In conclusion, integrating neem oil biodiesel with HCCI-DI combustion and  $Al_2O_3$  nano-additives offers a promising pathway to enhance engine performance and substantially lower emissions, advancing sustainable engine technology.

# Biyodizel–Dietil Eter–Nanoparçacık Karışımları ile Hibrit HCCI-DI Yanmasında Termal Verimlilik ve Emisyonların Optimizasyonu

## MAKALE BİLGİSİ

### Anahtar Kelimeler:

Neem yağı biyodizel  
HCCI-DI yanma  
Nano katkı maddesi  
Performans  
Emisyonlar

## ÖZET

Bu çalışma, fosil yakıtlara sürdürülebilir alternatiflere yönelik artan talep bağlamında, Homojen Karışım Sıkıştırılmalı Ateşleme–Doğrudan Enjeksiyon (HCCI-DI) motorunda nim yağı biyodizel karışımlarının yanma, performans ve emisyon özelliklerini inceleyerek, motor verimliliğinin optimize edilmesi ve çevresel etkinin azaltılmasını amaçlamaktadır. Çalışmanın önemi, alternatif yakıtlar ve ileri yanma stratejileri kullanılarak termal verimliliğin artırılması ve emisyonların en aza indirilmesi yönündeki iki temel zorluğun ele alınmasında yatmaktadır. Motor davranışı, biyodizel karışım oranları (B25, B50, B75, B100), yanma modları (DI ve HCCI-DI) ve 50 ppm alüminyum oksit ( $Al_2O_3$ ) nanoparçacık katkısının eklenmesi temelinde analiz edilmiştir. Elde edilen temel bulgular, biyodizel oranının artmasının hem DI hem de HCCI-DI modlarında silindiri içi maksimum basınç ( $P_{max}$ ) ve ısı salınım oranlarını azalttığını göstermektedir. DI moduna kıyasla HCCI-DI modu yanma karakteristiklerini iyileştirmiş; bu iyileşme  $Al_2O_3$  nanoparçacık katkısıyla daha da belirgin hale gelmiştir. Saf biyodizel (B100), dizel yakıtı kıyasla fren termal verimini (BTE) DI modunda %2,01, HCCI-DI modunda ise %1,68 oranında azaltmıştır. Bununla birlikte, HCCI-DI ve nanoparçacık katkısı, hem dizel hem de biyodizel karışımları için BTE değerlerini artırmıştır. Azot oksit ( $NO_x$ ) emisyonları B100 ile DI modunda %18,3 artarken, nanoparçacık katkılı HCCI-DI modunda %4,3 azalmıştır. Hidrokarbon (HC) emisyonları DI modunda biyodizel kullanımıyla %52,17 oranında düşmüş, ancak HCCI-DI modunda hafif bir artış göstermiştir; buna karşın nanoparçacık katkısı HC emisyonlarını %19,51'e kadar azaltmıştır. Karbon monoksit (CO) emisyonları %55,56'ya, duman emisyonları ise DI modunda %22,7'ye ve HCCI-DI modunda %39,1'e varan oranlarda azalmıştır. Sonuç olarak, nim yağı biyodizelinin HCCI-DI yanma modu ve  $Al_2O_3$  nanoparçacık katkısı ile entegre edilmesi, motor performansını iyileştirirken emisyonları önemli ölçüde azaltan sürdürülebilir motor teknolojisine doğru umut verici bir yaklaşım sunmaktadır.

## NOMENCLATURE

BTE	Brake thermal efficiency	FSN	Filter Smoke Number
CFD	Computational Fluid Dynamics	HCCI-DI	Homogeneous Charge Compression Ignition-Direct Injection
CI	Compression Ignition	HRR	Heat release rate
DI	Direct Injection	PAH	Polycyclic aromatic hydrocarbon
FAME	Fatty acid methyl esters	WCO	Waste Cooking Oil
FFA	Free fatty acids		

## INTRODUCTION

Developing sustainable and eco-friendly transportation solutions is necessary due to the transportation sector's substantial contribution to global energy consumption and greenhouse gas emissions (Vellaiyan et al., 2025a). A crucial role is played by Compression Ignition (CI) engines, which are widely used (Chen et al., 2024). CI engines enhance performance and environmental friendliness with advancements in alternative fuels, combustion technologies, and nanotechnology (Jayabal, 2024). CI engines can now benefit from new advancements in alternative fuels, combustion technologies, and nanotechnology, which enhance their performance and environmental friendliness (Zhu et al., 2025). In this study,  $Al_2O_3$  nano additives and HCCI-DI combustion modes are combined to study the synergistic effects on the engine using neem oil biodiesel blends (Veza et al., 2023).

Biodiesel can be made from fats and oils instead of petroleum-based diesel fuel (Jayabal, 2025). Neem oil, extracted from neem seeds, has garnered attention as a potential biodiesel feedstock since it is available, non-edible, and has favourable properties. *Azadirachta Indica* (Neem) is a versatile tree species native to the Indian subcontinent that serves many purposes, including medicinal, insecticidal, and agricultural purposes (Farokhi et al., 2023). There is a significant amount of oil in neem seeds, which ranges from 25% to 45%. The use of neem oil as a biodiesel feedstock has several benefits. Since it is non-edible, no food crops compete for agricultural land. As a sustainable source of oil, neem trees can grow on marginal or degraded lands. Furthermore, neem oil has a high cetane number, good oxidative stability, and a low point, all desirable properties for biodiesel.

Mathiyazhagan et al. examined an engine's production and emissions of neem biodiesel (Mathiyazhagan et al., 2022). Biodiesel was purified from unprocessed neem oil by acid-base catalysis. It was established that a mix of 20% neem biodiesel and diesel could reduce petroleum diesel consumption without adversely impacting the environment. Dash et al. investigated the neem seed oil synthesized into biodiesel, focusing on fuel properties and production optimization (Dash et al., 2021). For a biodiesel yield of 96%, the authors optimized the amount of catalyst, the speed, the temperature, and the reaction time. Experiments were conducted by Mohankumar et al. with neem oil biodiesel blending with ethanol (Mohankumar et al., 2023). Various proportions of neem oil, ethanol, and diesel were tested on an engine.

With advanced combustion technologies, such as HCCI, engine efficiency can be improved while emissions can be reduced. HCCI combustion involves the autoignition of a homogenized air-fuel mixture, which produces lower temperatures and fewer NOx (Zhang et al., 2025). Controlling HCCI combustion, however, remains a challenge. As a promising solution, the HCCI-DI combines the advantages of HCCI and DI. During the intake stroke, a portion of the fuel is injected, and the remainder is directly injected (Fang et al.,

2025). Leo et al. blended waste cooking oil (WCO) with  $Al_2O_3$  and nano ferric chloride ( $FeCl_3$ ) for use in HCCI-DI engines (Lionus Leo et al., 2024). Smoke, HC, and CO emissions from WCO declined significantly compared to pure diesel. BTE and NOx emissions were further improved by adding gasoline as a premix.  $FeCl_3$  and  $Al_2O_3$  also demonstrated promising results, with  $Al_2O_3$  improving BTE and reducing exhaust emissions, and  $FeCl_3$  decreasing HC and CO.

Spanò et al. studied the opportunity to improve the reactivity of mixtures and the expansion of their functional limit by using oxygen-enriched combustion in a methane-fuelled HCCI engine (Spanò et al., 2024). Experiments revealed that increasing oxygen content to 90% reduced the intake temperature requirement. Coskun et al. studied the combustion and emission characteristics of an HCCI-DI engine (Coskun et al., 2014). Validation of computational fluid dynamics (CFD) simulations was conducted against findings from experiments in the study that combined experimental and computational approaches. HCCI significantly reduced NOx emissions and decreased  $P_{max}$ . The CFD model was used to visualize the in-cylinder temperature and NOx of HCCI.

Nano additives have been explored to boost fuel characteristics (Zhang et al., 2025).  $Al_2O_3$  nanoparticles have received attention due to their excellent thermal stability, catalytic characteristics, and high surface area-to-volume ratio (Da Silva Medeiros et al., 2025). Iraqi diesel fuel was added with nano- $Al_2O_3$  and nano- $TiO_2$  in varying mass fractions by Dhahad et al. (Dhahad et al., 2020). Adding these nanomaterials increased the  $P_{max}$ , and ignition was significantly affected. A change from 18.9% to 24.25% and 20.45% was achieved for BTE when Nano- $TiO_2$  and Nano- $Al_2O_3$  were added to conventional diesel. Under maximum load conditions, the  $P_{max}$  was raised from 62 to 63.2 bar and 60.4 bar by adding nano- $Al_2O_3$  and nano- $TiO_2$  at 25 ppm.

Arif Savaş et al. investigated the performance and emission characteristics of a diesel engine using  $MgCO_3$  nanoparticle-doped jojoba biodiesel, optimized via Response Surface Methodology (RSM) (Savaş et al., 2025). Their study found that adding  $MgCO_3$  nanoparticles reduced CO and HC emissions while increasing NOx and  $CO_2$ , with optimal results at 74.20 ppm and 1.4 kW load, achieving a BTE of 23.67% and BSFC of 376.27 g/kWh. The RSM model demonstrated high accuracy, with  $R^2$  values above 95% and error rates below 10%. Ramazan Şener et al. explore the performance and emissions of a 20% waste cooking oil biodiesel blend (B20) in a compression ignition (CI) engine, compared to neat diesel (ŞENER, 2021). Experimental and CFD simulation results showed that B20 reduced CO emissions by 10.5%, NOx by 2.3%, and soot by 10.2%, while cylinder pressure dropped by 2.5%. Mahmut Beyaz et al. examine the impact of ethyl proxitol in biodiesel blends (E15B30 and E15B40) on a single-cylinder CI engine (Beyaz et al., 2025). The results showed improved combustion efficiency (higher CGP, HRR, and MGT) at medium and high loads, enhanced cold filter plugging point for better cold-weather performance, and maintained emission levels.

Simhadri et al. analyzed diesel engines using Mahua biodiesel blended with diesel (B20) and varying concentrations of nano TiO<sub>2</sub> at various injection pressures (Simhadri et al., 2024). TiO<sub>2</sub> was added to increase performance as the injection pressure increased. At 180 bars, B20T50 had similar combustion characteristics to diesel and a 5.3% higher heat release rate than B20 at low injection pressures. A fuel blend that contained TiO<sub>2</sub> also reduced CO and HC emissions. The fuel injection pressure of 240 bar resulted in the most significant reduction in smoke opacity and NO<sub>x</sub> emissions.

## Research Gap And Novelty

Previous research has individually explored biodiesel, HCCI-DI, and nano-additives. Still, no study has comprehensively integrated neem oil biodiesel blends, HCCI-DI combustion, and Al<sub>2</sub>O<sub>3</sub> nano-additives to assess their combined effects in a CI engine. Unlike focus on neem biodiesel in DI mode, WCO-based HCCI-DI without neem oil, this study leverages neem biodiesel's unique properties, HCCI-DI's efficiency-emission balance, and Al<sub>2</sub>O<sub>3</sub>'s catalytic enhancements. This synergy aims to enhance engine efficiency and reduce emissions beyond what individual technologies achieve, filling a critical gap in the literature.

This study analyzes combustion, performance, and emissions in a CI engine using neem biodiesel blends (B25, B50, B75, B100), comparing conventional DI and HCCI-DI modes, and evaluating Al<sub>2</sub>O<sub>3</sub> nano-additives' effects with diesel and biodiesel fuels. By elucidating these interactions, the research provides insights into designing efficient, low-emission CI engines, contributing to sustainable transportation and climate change mitigation through renewable fuels, advanced combustion, and nanotechnology.

## MATERIALS AND METHODS

### Fuel preparation

Mechanical pressing was used to extract neem oil, which was used as the primary feedstock in this study. To reduce the moisture content of the neem seeds, they were first cleaned and dried to remove any foreign matter. The dried seeds were then fed into a mechanical expeller, which applied high pressure to extract the oil. Separate discharges were made for the expelled oil and the remaining seed cake. As a result of its simplicity, environmental friendliness, and lack of chemical use, mechanical pressing was chosen as the extraction method. In producing biodiesel, crude neem oil was refined to remove impurities and contaminants that could interfere with the transesterification reaction. Crude neem oil was initially degummed to remove phospholipids, gums, and other gummy substances. A controlled temperature and agitation were used to treat the oil with water. Centrifugation was used to separate the oil from the hydrated gums and impurities. The degumming process improved the oil's stability and quality, allowing it to be further processed.

A neutralization process was then used to remove FFA from the degummed oil. In high FFA levels, soap can form during the transesterification reaction, reducing the yield and quality of biodiesel. A sodium hydroxide (NaOH) solution was applied to the degummed oil to form soaps. After settling, soap and alkali were removed from the neutralized oil with water. The FFA content was reduced by neutralizing the oil to below 0.5%, making it suitable for biodiesel production.

Bleaching was the final refining process to remove minor impurities and colour pigments from neutralized neem oil. Under controlled temperature and vacuum conditions, bleaching earth was applied to the oil. Adsorbents selectively removed impurities from the oil, resulting in a lighter-coloured, purified oil. After filtering out the spent bleaching earth, the bleached oil was ready for transesterification.

Biodiesel is produced by transesterifying refined neem oil, which converts its triglycerides into methyl esters of fatty acids. Methanol was used as the alcohol, and sulfuric acid (H<sub>2</sub>SO<sub>4</sub>) was used as the transesterification catalyst. The reaction was performed on a hotplate with a capacity of 2 litres and a magnetic stirrer. A transesterification reaction occurred at 65°C, just above the boiling point of methanol, with a 2-hour reaction time to allow equilibrium and a stirring speed of 600 rpm so that the oil and methanol phases could be effectively mixed and transferred. The mixture was placed in a separating flask on a stand for six hours to separate the mixture following the chemical reaction. A density difference between the denser glycerol and the lighter biodiesel phase resulted from gravity separation. A liquid biodiesel was then separated from the crude glycerol by draining it off.

**Table 1.** Fuel Properties

<i>Fuel Blend</i>	<i>Density (kg/m<sup>3</sup>), at 15°C</i>	<i>Kinematic Viscosity (mm<sup>2</sup>/s), at 40°C</i>	<i>Flash Point (°C)</i>	<i>Fire Point (°C)</i>	<i>Calorific Value (kJ/kg)</i>	<i>Cetane Number</i>
DEE	715	0.23	-41	-39	33,950	>100
Diesel (D)	821	2.43	53	56	42,467	50
D+Al <sub>2</sub> O <sub>3</sub> (50 ppm)	822	2.45	53	56	42,450	50
B25 (B25D75)	845	3.67	102	108	41,322	52
B50 (B50D50)	862	4.15	124	129	39,899	54
B75 (B75D25)	883	4.80	132	137	38,439	56
B100 (B)	911	5.44	150	158	36,984	58
B100+Al <sub>2</sub> O <sub>3</sub> (50 ppm)	912	5.46	150	158	36,970	58
Standard test method	ASTM D1298	ASTM D445	ASTM D93	ASTM D93	ASTM D240	ASTM D613

It was washed four times with warm water to remove residual catalysts, excess methanol, and glycerol from the separated biodiesel (40-50°C). A water and biodiesel mixture was gently mixed and separated during washing. Impediments were then discarded from the aqueous layer. Finally, the biodiesel was heated to 105°C in a hot air oven for 30 minutes to remove any remaining moisture. This step ensures that the biodiesel meets the moisture content requirements. Table 1 presents the fundamental fuel properties of the different fuel blends.

As per ASTM D613, the cetane numbers of diesel (D, CN=50) and pure neem oil biodiesel (B100, CN=58), using a CFR F5 Cetane Engine, have been measured. The engine was operated under standard conditions while the compression ratio was altered until ignition occurred, with a set delay, and the averages were taken over three runs for sophistication. The cetane numbers for the intermediate blends (B25, B50 and B75) were determined by linear interpolation between the measurements of D and B100, weighted according to their volumetric ratios. The cetane number for diethyl ether (DEE) was taken from the literature. DEE cetane number > 100 reflects a very good ignition quality, as reported in other studies. Due to DEE's high volatility, no direct measurement

was performed using ASTM D613. Still, the cited value indicates its superior ignitability relative to diesel and biodiesel.

In this study, a ball milling machine was used to prepare an Al<sub>2</sub>O<sub>3</sub> nano additive from micrometre-scale Al<sub>2</sub>O<sub>3</sub> powder, which was sourced from a supplier of chemical and laboratory products. A specific amount of the Al<sub>2</sub>O<sub>3</sub> powder was weighed and placed into the ball milling machine along with milling media, such as small steel balls. The milling process was initiated, exposing the powder and media to high-energy collisions and grinding forces. Over 10 hours, the micrometre-scale Al<sub>2</sub>O<sub>3</sub> particles were significantly reduced in size, resulting in nanoscale Al<sub>2</sub>O<sub>3</sub> particles. The rotational motion of the machine aided in breaking down and refining the particles, ultimately producing the desired nano additive. Once milling was complete, the Al<sub>2</sub>O<sub>3</sub> nano additive was carefully removed from the machine. Additional procedures, such as sieving or sonication, were applied to ensure consistent particle size and avoid clumping. The particle size of the nano additive was assessed using Scanning Electron Microscopy (SEM). Analysis of the SEM image (shown in Fig. 1) using ImageJ software revealed an average alumina nanoparticle size of 20.3 nm, providing insight into the morphology and structure of the nano additive. This small size ensures that the nanoparticles are much smaller than the injector nozzle's diameter, allowing them to pass through without obstructing the flow.

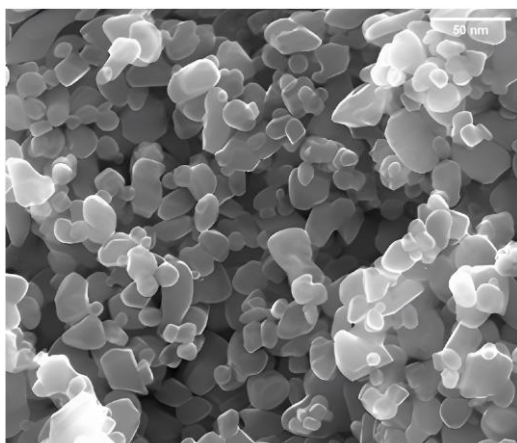


**Figure 1.** Scanning electron microscopy (SEM) image of Al<sub>2</sub>O<sub>3</sub> nano additive.

Fuel blends (B25, B50, B75, B100) were prepared by mixing neem oil biodiesel with diesel in volumetric ratios of 25:75, 50:50, 75:25, and 100:0, respectively, using a magnetic stirrer at 600 rpm for 30 minutes to ensure homogeneity. For nanoparticle addition, 50 ppm of Al<sub>2</sub>O<sub>3</sub> nanoparticles were incorporated into diesel (D) and biodiesel (B100) blends. The nanoparticles were dispersed using an ultrasonicator (frequency 40 kHz) for 30 minutes at ambient temperature to achieve uniform suspension. The choice of 50 ppm was based on prior studies indicating an optimal balance between combustion enhancement and agglomeration prevention, as higher concentrations (e.g., >100 ppm) may lead to nanoparticle clustering, reducing effectiveness.

To investigate the effect of nanoparticles, 50 ppm of Al<sub>2</sub>O<sub>3</sub> nanoparticles were blended into the diesel (D) and biodiesel (B100) fuels using an ultrasonicator for 30 minutes to ensure uniform dispersion. The addition of Al<sub>2</sub>O<sub>3</sub> nanoparticles slightly increases the density and viscosity of the blends due to the solid particulate matter. At the same time, the calorific value may marginally decrease due to the non-combustible nature of the nanoparticles.

## Engine setup

The schematic diagram in Fig. 2 shows the experimental setup for investigating neem oil biodiesel blend characteristics in HCCI-DI engines. In the experiment, a single-cylinder CI engine is modified to combine HCCI and DI modes with a dual-fuel system. In the DI mode, neem oil biodiesel and diesel are blended with 50 ppm Al<sub>2</sub>O<sub>3</sub> nano additive. In the HCCI mode, diethyl ether (DEE) is introduced through a separate fuel injector in the inlet manifold. A mixture ratio of 20% HCCI and 80% DI is used, and an engine speed of 1500 rpm is maintained. Inlet manifold HCCI fuel injection occurs during the intake stroke, while DI fuel injection occurs 23° before Top Dead Center (bTDC).

The experimental setup includes a separate fuel tank for DEE and an electronic control unit that regulates fuel supply and fuel injection timing. An electrical swingfield dynamometer measures the engine's performance. At various points in the system, thermocouples are strategically placed to monitor the temperature, and a U-tube manometer measures the pressure drop across the intake airflow. A surge tank is incorporated to dampen pressure fluctuations in the intake system.

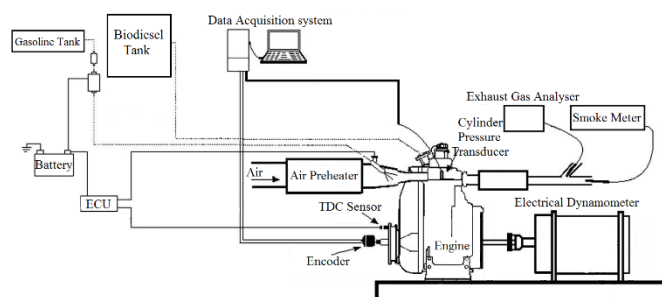


**Figure 2.** Schematic view of the experiment.

**Table 2.** Fuel Properties

Description	Details
Model of the engine	Natural-aspiration single-cylinder engine
Power rated	4.4 kW
Speed rated	1500 RPM
Ratio of compression	17.5:1
Bore	87.5 mm
Stroke	110 mm
DI fuel injection timing	23° before TDC

**Table 3.** Instrument ranges, accuracy percentages, and uncertainty percentages

Instrument	Measurement range	Accuracy	Uncertainty percentage
AVL DI GAS 444 five-gas analyzer			
NO <sub>x</sub>	(0-5000 ppm vol)	<500ppm vol: ± 50ppm vol	± 0.25
		>500ppm vol: ± 10%	
HC	(0-20000 ppm vol)	<200ppm vol: ± 10ppm vol	± 0.2
		>200ppm vol: ± 5%	
CO	(0-10% vol)	<0.6% vol: ± 0.03% vol	± 0.35
		>0.6% vol: ± 5%	
CO <sub>2</sub>	(0-20% vol)	<10% vol: ± 0.5% vol	± 0.2
		>10% vol: ± 5%	
O <sub>2</sub>	(0-22% vol)	<2% vol: ± 0.1% vol	± 0.35
		>2% vol: ± 5%	
AVL 415 smoke meter			
Smoke Intensity	0 to 10 FSN	0.002 FSN	± 1

A Piezoelectric Pressure Transducer AVL GH14D/AH01 uses an AVL 365C encoder to measure the in-cylinder pressure at every crank angle interval of 0.5°. A total of 50 subsequent measurements are collected to ensure accuracy and consistency. A five-gas analyzer (AVL DI GAS 444) is used to analyze exhaust emissions, measuring CO, CO<sub>2</sub>, HC, NO<sub>x</sub>, and oxygen (O<sub>2</sub>). Smoke from the engine is also calculated using an AVL 415 smoke meter. Table 2 provides detailed engine specifications used in this experimental study. Table 3 presents a list of the instruments employed in the study, along with their respective measurement ranges, accuracies, and uncertainty percentages.

## Experimental Procedure

Initially, the engine was operated at 1500 rpm to reach steady-state operating conditions. Inlet manifold HCCI fuel injection occurs during the intake stroke, while DI fuel injection occurs at 23° bTDC. The electronic control unit adjusts the fuel mixture ratio to 20% HCCI and 80% DI. The data acquisition process is initiated once the engine reaches stable operating conditions, recording in-cylinder pressure, crank angle, and other relevant parameters for 50 successive engine cycles. With the gas analyzer and smoke meter, exhaust emissions are measured simultaneously. Using EngineSoft software, the acquired data from 50 consecutive cycles are processed to calculate the average values of in-cylinder pressure, HRR, and other combustion parameters. The emission data is analyzed and compared with the baseline data.

## RESULTS AND DISCUSSION

### Combustion Characteristics

#### In-cylinder pressure

To gain insights into the combustion process and engine performance, the pressure data were plotted against the crank angle. A key parameter derived from these pressure curves is the  $P_{max}$ , representing the maximum pressure reached during combustion. It is a crucial indicator of the engine's performance since it directly influences its power output, efficiency, and emissions [1].  $P_{max}$  values are compared for different fuel blends and combustion modes, with and without nano additive, to evaluate biodiesel content and nano additive's influence on combustion and performance [2].

Figure 3 shows in-cylinder pressure variations for different fuel blends and combustion modes. In the DI fuel blends without nano additives, pure diesel exhibits a significantly higher  $P_{max}$  than pure biodiesel. Pure biodiesel has a  $P_{max}$  that is 2.17% lower than pure diesel. Biodiesel has a lower energy density than diesel. Due to this, diesel will release more energy during combustion for the same volume of fuel injected (Bhikuning et al., 2022; Tai et al., 2023; Y. Zhang et al., 2021). As a result of its lower energy density, biodiesel has a lower  $P_{max}$  than diesel. The cetane number of biodiesels is lower than that of diesel. When exposed to the high temperatures and pressures of combustion chambers, fuel with a higher cetane number will ignite more readily (Yasar et al., 2022). The longer ignition delay is associated with diesel fuel; the faster its pressure rises, and its peak pressure is higher than that of biodiesel. Compared to diesel, biodiesel is viscous, which may impact atomization and mixing. As biodiesel has a higher viscosity, larger fuel droplets may form

during injection and combustion, and the fuel may not mix well with air.

Compared to diesel, this can result in a slower combustion rate and fewer peak pressures (Vellaiyan et al., 2025b). Diesel primarily comprises hydrocarbons, while biodiesel contains oxygen in its molecular structure. As oxygen is present in biodiesel, it can lead to complete combustion (Sekar et al., 2021). A portion of the mass of biodiesel, however, is occupied by oxygen atoms rather than energy-rich hydrocarbons, which reduces its overall energy content. With biodiesel, peak pressures are lower compared to diesel because of this. Combining these factors results in a 2.17% reduction in peak pressure when comparing pure biodiesel and pure diesel in DI fuel blends without nano additives. Pure diesel has a higher  $P_{max}$  due to its superior energy content, better ignition quality, and better physical properties than pure biodiesel.

Compared to DEE-D, the  $P_{max}$  of DEE-B is 1.23% lower. A combination of fuel properties and the HCCI combustion mode accounts for this difference in peak pressure. HCCI-DI mode without nano additive results in 1.23% less peak pressure with biodiesel over diesel due to the interaction of energy density, cetane number, viscosity, and oxygen content.

HCCI-DI mode results in higher  $P_{max}$  for diesel and biodiesel than the DI mode without nano additives. The  $P_{max}$  for diesel in HCCI-DI mode (DEE-D) is 65.622 bar, which is 2.46% higher than the 64.046 bar in DI mode. Biodiesel also has a  $P_{max}$  of 64.815 bar in HCCI-DI mode, which is 3.45% higher than 62.654 bar in DI mode. An injection of fuel during the intake stroke creates a homogeneous mixture, promoting autoignition in HCCI-DI. As a result, combustion is faster and more simultaneous than DI-only operations. DEE's high cetane number allows it to ignite readily in a combustion chamber with high temperatures and pressures. HCCI-DI mode speeds up combustion and ensures simultaneous combustion throughout the chamber. DEE injection produces a homogeneous mixture, which results in faster combustion due to a more uniform distribution of fuel (Mishra et al., 2024). As a result of rapid combustion, the HCCI-DI mode exhibits higher peak pressures than the DI mode. Fuel and air are mixed more effectively with DEE injected during the intake stroke (Jairam et al., 2021). Compared to DI-only operation, where mixing time is limited, the homogeneous DEE mixture promotes better air-fuel mixing. HCCI-DI mode achieves more efficient combustion due to improved mixing.

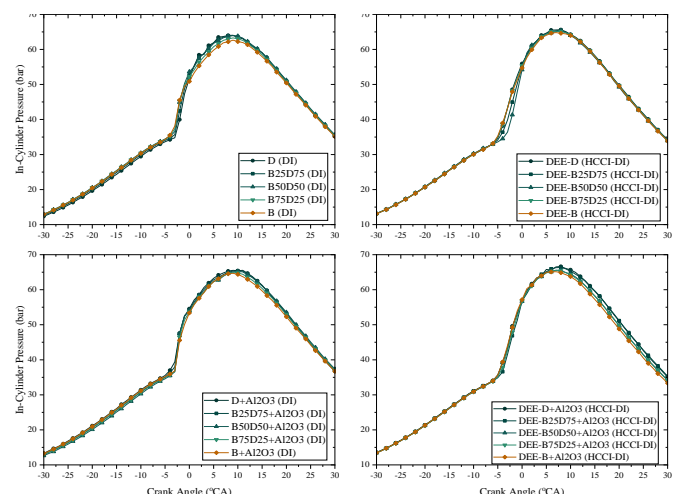


Figure 3. Variations in-cylinder pressure for different fuel blends, combustion modes, and Al<sub>2</sub>O<sub>3</sub> nano additive.

In HCCI-DI and DI modes, adding Al<sub>2</sub>O<sub>3</sub> nano additive significantly affects P<sub>max</sub>. By adding Al<sub>2</sub>O<sub>3</sub> nano additive to diesel in DI mode, P<sub>max</sub> increased by 2.34% from 64.046 bar without the nano additive (D) to 65.543 bar with the nano additive (D+Al<sub>2</sub>O<sub>3</sub>). The nano Al<sub>2</sub>O<sub>3</sub> increases P<sub>max</sub> by 1.52% in HCCI-DI mode, going from 65.622 bar without it (DEE-D) to 66.619 bar with it (DEE-D+Al<sub>2</sub>O<sub>3</sub>). By adding Al<sub>2</sub>O<sub>3</sub> nano additive to biodiesel in DI mode, P<sub>max</sub> increases by 3.23%, from 62.654 bar without the nano additive to 64.683 bar with the nano additive (B+Al<sub>2</sub>O<sub>3</sub>). Upon adding Al<sub>2</sub>O<sub>3</sub> to biodiesel in HCCI-DI mode, P<sub>max</sub> increases by 0.52% from 64.815 bar without the nano additive (DEE-B) to 65.149 bar (DEE-B+Al<sub>2</sub>O<sub>3</sub>).

Peak pressure from the combustion of Al<sub>2</sub>O<sub>3</sub> nano additives varies according to the fuel and combustion mode. Diesel (2.34%) and biodiesel (3.23%) experience significant increases in P<sub>max</sub> when the nano additive is used in DI mode. The nano additive's ability to improve fuel properties, such as enhanced ignition characteristics, faster combustion rates, and increased heat release, can be attributed to the nano additive's ability to improve fuel properties (Jokubynienė et al., 2023). Al<sub>2</sub>O<sub>3</sub> nanoparticles are added as catalysts in the fuel, accelerating combustion and enhancing peak pressure. Both diesel and biodiesel benefit from the nano additive in HCCI-DI mode, increasing P<sub>max</sub> by 1.52% and 0.52%, respectively. As a result of the combined effects of the nano additive and the HCCI combustion process, a more homogeneous and efficient combustion occurs. With the nano additive in HCCI-DI mode for biodiesel, the modest increase in P<sub>max</sub> (0.52%) suggests that the Al<sub>2</sub>O<sub>3</sub> nanoparticles synergize with biodiesel's unique properties, such as its higher oxygen content. In HCCI-DI mode, the nano additive slightly enhances biodiesel's autoignition behaviour, HRR, and combustion efficiency, increasing peak pressure.

### Heat release rate

An HRR reveals valuable insights into combustion processes and the efficiency of internal combustion engines. HRR measures the chemical energy a fuel releases during combustion, directly affecting engine performance, emissions, and efficiency. Therefore, it is essential to investigate the HRR characteristics of different fuels and combustion modes. The HRR is calculated by analyzing the in-cylinder pressure data obtained from engine experiments. Equation (1) shows the HRR equation using the first law of thermodynamics.

$$\frac{dQ}{d\theta} = \left(\frac{\gamma}{\gamma-1}\right) \times p \times \frac{dV}{d\theta} + \left(\frac{1}{\gamma-1}\right) \times V \times \left(\frac{dp}{d\theta}\right) \quad (1)$$

Where dQ/dθ is HRR (J/°CA), γ is specific heat ratio, p is in-cylinder pressure (Pa), V is cylinder volume (m<sup>3</sup>), and θ is the crank angle (°CA).

HRR is shown in Fig. 4 for different fuel blends. Diesel, B25D75, B50D50, B75D25, and B100 have HRR<sub>max</sub> values of 53.024 J/°CA, 52.088 J/°CA, 51.232 J/°CA, 46.925 J/°CA, and 42.619 J/°CA, correspondingly. In comparison with diesel, the HRR<sub>max</sub> values of B25D75, B50D50, B75D25, and B100 decreased by 1.76%, 3.38%, 11.51%, and 19.63%, respectively. Neem oil biodiesel contributes to a decrease in HRR<sub>max</sub> when its proportion is higher in the blend. Compared with diesel, biodiesel's viscosity and volatility

are higher, which causes it to burn more slowly and release less heat (Mohanrajhu et al., 2024). The HRR profiles for diesel and neem biodiesel are different. The HRR of diesel fuel increases sharply during premixed combustion and then rapidly decreases during diffusion combustion (Sheik et al., 2024). However, biodiesel blends exhibit a slower decrease in HRR during diffusion than premixed. The oxygen content in biodiesel makes it, and heat is released at a higher rate and longer than gasoline (Lionus Leo et al., 2025a). As biodiesel is viscous-based and has a lower calorific value than petroleum diesel, it burns more slowly. It produces a lower peak HRR than diesel due to the longer combustion duration and lower combustion temperature.

Compared to diesel, biodiesel blends have an earlier start of combustion (SOC). HRR values for biodiesel blends increase swiftly at an earlier crank angle, confirming this observation. In biodiesel blends, an increased oxygen content facilitates combustion and increases ignition speed, which increases SOC earlier (). The sustained HRR profiles for biodiesel blends over diesel show a longer combustion duration. Having low volatility and viscosity, biodiesel has an extended combustion duration because it burns more slowly (G M et al., 2023).

DEE-D and DEE-B have HRR<sub>max</sub> values of 57.939 J/°CA and 54.663 J/°CA, respectively. HRR<sub>max</sub> decreased by 5.66% for DEE-B compared to DEE-D. The lower volatility and viscosity of biodiesel result in a slower combustion rate, which results in a lower HRR<sub>max</sub>. Biodiesel's lower calorific value results in lower HRR<sub>max</sub> (Subramani et al., 2020).

Experimental results demonstrate that DI and HCCI-DI modes for diesel and biodiesel have different HRR characteristics. In DI mode, diesel and neem biodiesel have HRR<sub>max</sub> values of 53.024 J/°CA and 42.619 J/°CA, respectively. DEE-D and DEE-B have HRR<sub>max</sub> values of 57.939 J/°CA and 54.663 J/°CA, respectively, in HCCI-DI mode. The HRR<sub>max</sub> values for diesel increased by 9.27% from D to DEE-D when comparing DI and HCCI-DI, whereas the HRR<sub>max</sub> values for biodiesel increased by 28.26% when comparing B to DEE-B when comparing DI and HCCI-DI. As a result of the premixed charge, HRR<sub>max</sub> values are higher in HCCI-DI. By injecting DEE at the port, HCCI combustion enhances the overall combustion process, resulting in higher HRRs than conventional DI combustion.

The HRR profiles of diesel and biodiesel in DI mode show premixed and diffusion combustion phases. The premixed combustion phase of DEE-D and DEE-B is more pronounced in the HCCI-DI mode, with higher HRR peaks. Having DEE injected at the port promotes a more homogeneous air-fuel mixture, leading to faster and more intense combustion. HCCI-DI mode also shows longer combustion durations than DI mode, suggesting a longer combustion process for DEE-D and DEE-B. DEE-D and DEE-B exhibit an earlier SOC in HCCI-DI than in DI. A more reactive mixture is created by injecting DEE at the port, resulting in an advanced SOC (Al-Dawody et al., 2021). Biodiesel has a slower combustion rate than gasoline, compensated by the earlier SOC in HCCI-DI mode. Hence, a more complete combustion is achieved within the available period with HCCI-DI. In HCCI-DI mode, despite a longer combustion duration, a higher SOC ensures efficient combustion.

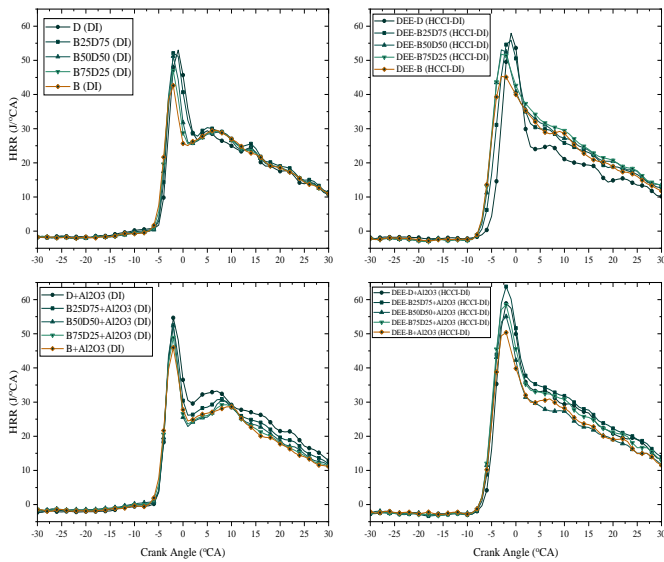


**Figure 4.** Variations of HRR for different fuel blends, combustion modes, and  $\text{Al}_2\text{O}_3$  nano additive.

In both DI and HCCI-DI modes,  $\text{Al}_2\text{O}_3$  nano additive significantly affects HRR characteristics of diesel and biodiesel (B). Using DI mode, D and B have HRRmax values of 53.024 J/°CA and 42.619 J/°CA, respectively, while D+ $\text{Al}_2\text{O}_3$  and B+ $\text{Al}_2\text{O}_3$  have HRRmax values of 54.663 J/°CA and 54.662 J/°CA, respectively. Diesel HRRmax increases by 3.09%, and biodiesel HRRmax increases by 28.26% when  $\text{Al}_2\text{O}_3$  nano additives are used in DI mode. The HRRmax values for DEE-D and DEE-B in HCCI-DI mode are 57.939 J/°CA and 54.663 J/°CA, respectively, while for DEE-D+ $\text{Al}_2\text{O}_3$  and DEE-B+ $\text{Al}_2\text{O}_3$ , they are 58.884 J/°CA and 58.884 J/°CA, respectively. Diesel HRRmax increases by 1.63%, and biodiesel HRRmax increases by 7.74% with  $\text{Al}_2\text{O}_3$  nano additive in HCCI-DI mode. As a result of the  $\text{Al}_2\text{O}_3$  nanoparticles, enhanced combustion efficiency is achieved through improved fuel atomization, evaporation, and mixing processes (Bazdidi-Tehrani et al., 2023). Moreover, the nanoparticles act as catalysts, allowing the combustion process to proceed more efficiently. When diesel and biodiesel are run in HCCI-DI mode, the HRR curves display higher peaks and shorter combustion durations than diesel and biodiesel without  $\text{Al}_2\text{O}_3$  nano additives. Nano additives enhance the homogeneity of the air-fuel mix and speed up chemical reactions in HCCI combustion (Venkatesan & Kadiresh, 2015).

### Brake thermal efficiency

Figure 5 displays thermal efficiency variations for different fuel blends, combustion modes, and the presence or absence of nano  $\text{Al}_2\text{O}_3$ . Diesel has the highest BTE at maximum load when compared with various blends of biodiesel containing neem oil. The BTE decreases with increasing neem oil biodiesel proportions, with B25D75 at 29.17%, B50D50 at 28.47%, B75D25 at 28.17%, and B100 at 27.87%. Compared to diesel, biodiesel has a lower energy content, meaning less energy is released from combustion, thus reducing the BTE. Due to its higher viscosity, biodiesel is less atomized and mixes with air poorly, which causes incomplete combustion and reduces BTE. Furthermore, as biodiesel contains oxygen while improving combustion efficiency, it also reduces the fuel's energy content, resulting in lower BTE. The higher specific gravity of biodiesel decreases combustion efficiency due to its effects on the fuel injection process (Madihi et al., 2022).

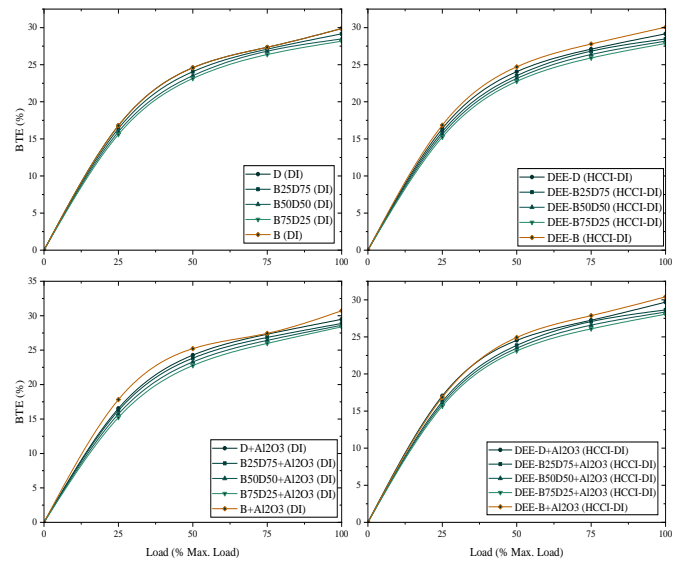


**Figure 5.** Variations of thermal efficiency for different fuel blends, combustion modes, and  $\text{Al}_2\text{O}_3$  nano additive

At maximum load, HCCI-DI mode without  $\text{Al}_2\text{O}_3$  nano additive for diesel and neem oil biodiesel blends showed a similar trend to DI mode. The highest BTE was recorded by DEE-D, followed by DEE-B25D75 at 28.89%, DEE-B50D50 at 28.31%, DEE-B75D25 at 28.06%, and DEE-B at 27.82%. HCCI-DI mode has the same reduction in BTE with increasing biodiesel content as DI mode because biodiesel is lower in energy, has greater viscosity, has more oxygen content, and has higher specific gravity than diesel. The highest BTE is recorded by DEE-D at 30.06%, followed by DEE-B25D75 at 29.47%, DEE-B50D50 at 28.88%, DEE-B75D25 at 28.62%, and DEE-B at 28.38%. Biodiesel's lower calorific value, higher viscosity, higher oxygen content, and higher specific gravity can contribute to the decrease in BTE with increasing biodiesel content in the HCCI-DI (Shivkumar et al., 2021).

In HCCI-DI without  $\text{Al}_2\text{O}_3$  nano additive, diesel and B100 exhibit higher BTE values than in DI mode without  $\text{Al}_2\text{O}_3$ . The BTE of diesel in DI mode is 29.88%, whereas the BTE of DEE-D is 30.06%. In DI mode, B100 has a BTE of 27.87%, while DEE-B has a BTE of 28.38%. In HCCI combustion, fuel is injected during intake, mixed with air, and then compressed and ignited automatically. Due to the homogeneous charge, combustion efficiency is higher, and BTE is improved compared to the DI mode (SivaPrasad et al., 2022). Since DEE has a high latent heat of vaporization, DEE can diminish heat transfer losses and contribute to improved BTE during intake and compression strokes (Varpe & Kharde, 2023).

DEE, compared to diesel and biodiesel, also has higher volatility and lower viscosity, facilitating atomization and mixing fuel with air. Improved atomization and mixing further enhance HCCI-DI mode combustion efficiency and BTE. When HCCI-DI is used, partial fuel injection occurs during the intake stroke, which can reduce pumping losses compared to DI, which injects fuel during the compression stroke (Leo et al., 2021). As a result of the reduced pumping losses in the HCCI-DI mode, the observed BTE values are also higher.

In both DI and HCCI-DI modes at maximum load,  $\text{Al}_2\text{O}_3$  nano additive improves BTE in diesel and B100 when added to diesel and B100. A BTE of 30.73% is achieved in the DI mode with diesel plus  $\text{Al}_2\text{O}_3$ , compared with 29.88% for pure diesel. Similarly, B100 with  $\text{Al}_2\text{O}_3$  (B+ $\text{Al}_2\text{O}_3$ ) has a BTE of 28.06%, which is higher than pure B100 (B) at 27.87%. HCCI-DI has

DEE-D+Al<sub>2</sub>O<sub>3</sub> with a BTE of 30.40%, higher than DEE-D at 30.06%, and DEE-B+Al<sub>2</sub>O<sub>3</sub> with a BTE of 28.39%, higher than DEE-B. Adding Al<sub>2</sub>O<sub>3</sub> nanoparticles to the fuel makes the mixture more thermally conductive and has a more significant heat transfer coefficient. As a result of this improved heat transfer, combustion is more efficient, and BTE is improved. As an active catalyst, Al<sub>2</sub>O<sub>3</sub> nanoparticles boost fuel oxidation, reducing soot and unburned hydrocarbon formation during combustion. The catalytic effect contributes to improved combustion efficiency and higher BTE. Al<sub>2</sub>O<sub>3</sub> nanoparticles in fuel improve the atomization and uniformity of fuel-air mixing by modifying their surface tension and viscosity (Mary et al., 2023). As a result of this enhanced atomization, combustion is more efficient, and BTE is higher. Al<sub>2</sub>O<sub>3</sub> reduces the ignition delay period because it acts as a hot spot and promotes a faster ignition process. Shorter ignition delays lead to improved combustion phasing and BTE.

## Emission characteristics

### NO<sub>x</sub> emissions

Smog, acid rain, and tropospheric ozone are all caused by nitrogen oxides (NO<sub>x</sub>), a group of highly reactive gases. Industrial processes and internal combustion engines are the primary sources of NO<sub>x</sub> emissions. Due to its environmental and health effects, NO<sub>x</sub> formation in internal combustion engines is a significant concern. Globally, strict emission regulations have resulted in researchers developing innovative strategies to reduce NO<sub>x</sub> emissions.

A combination of thermal NO<sub>x</sub>, prompt NO<sub>x</sub>, and fuel NO<sub>x</sub> is the engine's primary source of NO<sub>x</sub> formation. Thermal NO<sub>x</sub>, governed by the Zeldovich mechanism, occurs during high-temperature combustion processes above 1,800 K, where nitrogen and oxygen molecules in the combustion air react. The reaction rate depends on peak combustion temperature and the residence time of gases at these elevated temperatures. Prompt NO<sub>x</sub>, described by the Fenimore mechanism, forms when nitrogen reacts rapidly with hydrocarbon radicals in the flame front, predominantly under fuel-rich conditions. Fuel NO<sub>x</sub> arises from the oxidation of nitrogen-containing compounds in fuels like coal or heavy oils (e.g., pyridine, quinoline). However, it is less significant for diesel and biodiesel, which typically contain minimal nitrogen. In this study, thermal NO<sub>x</sub> is the dominant contributor due to the high-temperature conditions in HCCI-DI and DI combustion.

Figure 6 shows the NO<sub>x</sub> for various fuel blends, combustion modes, and the presence or absence of Al<sub>2</sub>O<sub>3</sub> nano additive. It is evident from a comparison of neem oil biodiesel blends with and without the Al<sub>2</sub>O<sub>3</sub> nano additive that biodiesel fuels produce higher NO<sub>x</sub> emissions as the amount of biodiesel increases. This trend can be observed in all load conditions, but the difference is more pronounced at higher loads. At maximum load, neat diesel emitted 1009 ppm of NO<sub>x</sub>, whereas B25D75, B50D50, B75D25, and neat biodiesel emitted 1030, 1073, 1121, and 1194 ppm of NO<sub>x</sub>, respectively. Compared to neat diesel, these values represent an increase of 2.1%, 6.3%, 11.1%, and 18.3% in NO<sub>x</sub> emissions. The additional oxygen in biodiesel makes combustion more complete, causing higher temperatures in the cylinder. The increased NO<sub>x</sub> associated with biodiesel

blend combustion results from the elevated temperatures resulting from the combustion. Biodiesel has a chemical structure and properties different from conventional diesel. Higher cetane reduces biodiesel ignition delay. Due to a reduced ignition delay, combustion begins earlier, allowing NO<sub>x</sub> precursors to form more quickly. Biodiesel also exhibits poorer atomization and larger fuel droplets due to its higher viscosity and surface tension than diesel. The larger droplets cause localized hot spots during combustion, increasing NO<sub>x</sub> emissions (Liao et al., 2024).

Compared to the DI mode, DEE significantly reduces NO<sub>x</sub> emissions when used as the HCCI fuel in the HCCI-DI mode without the Al<sub>2</sub>O<sub>3</sub> nano additive. NO<sub>x</sub> emissions increase with increased biodiesel content; this also applies to DEE-biodiesel blends with increased biodiesel content. In DEE-B25D75, DEE-B50D50, and DEE-B75D25, NO<sub>x</sub> emissions were 986 ppm, 1034 ppm, and 1101 ppm, respectively. Compared to DEE-D, which emitted 966 ppm, these values represent an increase of 2.1%, 7.0%, and 14.0% in NO<sub>x</sub> emissions.

As a result of the HCCI-DI mode, both diesel and biodiesel produced less NO<sub>x</sub> than the DI mode. DEE-B emitted 1157 ppm of NO<sub>x</sub> at maximum load, a 3.1% reduction compared to biodiesel, which emitted 1194 ppm. The lower NO<sub>x</sub> emissions in HCCI-DI mode are attributed to a more uniform temperature distribution within the cylinder caused by the uniform mixing of DEE and air. With lean homogeneous combustion, NO<sub>x</sub> is suppressed due to lower peak temperatures. When HCCI-DI combustion is used with biodiesel, NO<sub>x</sub> emissions from neat biodiesel are reduced by a more significant percentage than those from diesel combustion (L. Zhang et al., 2023).

D+Al<sub>2</sub>O<sub>3</sub> in DI mode increased NO<sub>x</sub> emissions by 9.8% compared to neat diesel (D) with 50 ppm Al<sub>2</sub>O<sub>3</sub> nano additive. D+Al<sub>2</sub>O<sub>3</sub> emitted 1108 ppm of NO<sub>x</sub> during maximum load conditions, whereas diesel emitted 1009 ppm. Similarly, the Al<sub>2</sub>O<sub>3</sub> nano additive in the DI mode resulted in a 7.0% increase in NO<sub>x</sub> emissions when added to neat biodiesel (B+Al<sub>2</sub>O<sub>3</sub>). There were 1278 ppm of NO<sub>x</sub> emitted by B+Al<sub>2</sub>O<sub>3</sub>, while 1194 ppm of NO<sub>x</sub> were emitted by biodiesel. In HCCI-DI mode, the Al<sub>2</sub>O<sub>3</sub> nano additive caused a 4.0% rise in NO<sub>x</sub> emissions over DEE-D. DEE-D+Al<sub>2</sub>O<sub>3</sub> emits 1005 ppm of NO<sub>x</sub>, while DEE-D emits 966 ppm.

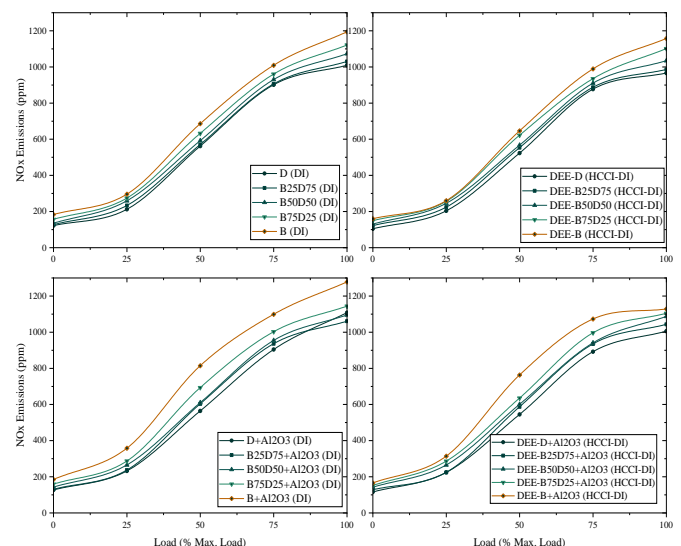


**Figure 6.** Variations of NO<sub>x</sub> emissions for different fuel blends, combustion modes, and Al<sub>2</sub>O<sub>3</sub> nano additive

Due to the increased surface area available for heat transfer and catalytic activity,  $\text{Al}_2\text{O}_3$  nanoparticles enhance a fuel's combustion properties. This results in more complete combustion, higher combustion temperatures, and, consequently, more  $\text{NO}_x$  emissions. Due to the nano  $\text{Al}_2\text{O}_3$ , the fuel ignites earlier in the combustion cycle due to the shorter ignition delay period (Leo et al., 2020). Since  $\text{NO}_x$  formation is highly dependent on the time spent at high temperatures, earlier combustion results in a longer residence time for  $\text{NO}_x$  formation. The  $\text{Al}_2\text{O}_3$  nanoparticles also increase oxygen availability during combustion.  $\text{NO}_x$  formation is strongly associated with oxygen availability at high temperatures, so an increase in oxygen content results in more  $\text{NO}_x$  emission.  $\text{Al}_2\text{O}_3$ 's high thermal conductivity enhances heat transfer within the combustion chamber. As a result of improved heat transfer, local temperatures can rise, causing  $\text{NO}_x$  to form more readily.

### HC emissions

Figure 7 illustrates the variations in HC for different fuel blends, combustion modes, and the presence or absence of  $\text{Al}_2\text{O}_3$  nano additive. When the biodiesel proportion increased, HC emissions decreased in the DI mode without a nano additive. For diesel, B25D75, B50D50, B75D25, and B100, HC emissions were 23ppm, 20ppm, 16ppm, 13ppm, and 11ppm, respectively, at maximum load. For B25D75, B50D50, B75D25, and biodiesel, HC emissions were reduced by 13.04%, 30.43%, 43.48%, and 52.17%, respectively. Higher oxygen levels in biodiesel promote a more complete combustion, which reduces HC emissions as biodiesel content increases. Furthermore, biodiesel is less volatile than diesel, which reduces HC emissions (Lionus Leo et al., 2025b).

It has also been shown that HC emissions in HCCI-DI mode decrease with biodiesel addition to the blend. DEE-D showed 41 ppm, DEE-B25D75, DEE-B50D50, DEE-B75D25, and DEE-B showed 38 ppm, 37 ppm, 34 ppm, and 32 ppm of HC emissions, respectively. The HC emissions of DEE-B25D75, DEE-B50D50, DEE-B75D25, and DEE-B decreased by 7.32%, 9.76%, 17.07%, and 21.95%, respectively, as compared to DEE-D. HC is reduced with increasing biodiesel content in the HCCI-DI mode for the same reasons as in the DI mode. Biodiesel has higher oxygen, lower volatility, and a higher cetane rating. This results in a more complete combustion and reduced HC emissions.

HCCI-DI mode produces higher HC emissions for diesel and biodiesel than DI mode without nano additive for both fuels when compared to DI mode without nano additive. At maximum load, the HC for diesel in DI and HCCI-DI are 23 ppm and 41 ppm, respectively. The HC emissions from biodiesel in DI and HCCI-DI modes are 11 and 32 ppm, respectively. In HCCI-DI mode, more HC is released from the DEE introduction during the intake stroke. As DEE vaporizes rapidly, it can cool the in-cylinder charge due to its high latent heat of vaporization. Effects of cooling can lead to locally rich regions and incomplete combustion, which increases HC emissions. HCCI-DI also lowers combustion temperature compared to DI, owing to the homogeneous mixture, contributing to higher HC emissions (Lionus Leo et al., 2018).

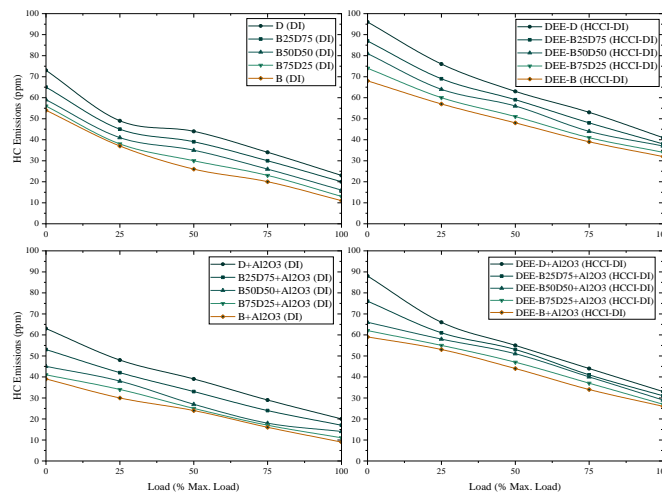


**Figure 7.** Variations of HC emissions for different fuel blends, combustion modes, and  $\text{Al}_2\text{O}_3$  nano additive

Nano additives  $\text{Al}_2\text{O}_3$  reduce HC emissions significantly in both DI and HCCI-DI modes for diesel and biodiesel. Without nano additives, diesel and biodiesel emit 23 ppm and 11 ppm of HC in DI mode. HC has dropped to 20 ppm for diesel and 9 ppm for biodiesel when  $\text{Al}_2\text{O}_3$  is added. This corresponds to a 13.04% reduction for diesel and an 18.18% reduction for biodiesel. Diesel and biodiesel emit 41 and 32 ppm HC without nano additives in HCCI-DI mode, respectively. HC emissions fall to 33 ppm for diesel and 26 ppm for biodiesel at maximum load when  $\text{Al}_2\text{O}_3$  is added. The reduction for diesel is 19.5%, and the reduction for biodiesel is 18.75%.

$\text{Al}_2\text{O}_3$  nano additive reduces HC emissions due to its catalytic effect and physicochemical properties. HC emissions can be reduced, and combustion can be completed more efficiently by  $\text{Al}_2\text{O}_3$  nanoparticles with high surface-to-volume ratios and enhanced reactivity. Nanoparticles of  $\text{Al}_2\text{O}_3$  act as catalysts in combustion chambers, speeding up the oxidation process (Mary et al., 2023). As a result of their presence, these nanoparticles provide additional active sites for oxygen adsorption and dissociation. By dissociating oxygen molecules, fuel molecules more readily react with oxygen atoms, promoting complete combustion. This catalytic effect reduces emissions. The area-to-volume ratio of  $\text{Al}_2\text{O}_3$  nanoparticles is significantly higher. With the increased surface area, fuel and oxygen molecules are more likely to adsorb, increasing the probability of their interaction and oxidation. The greater the surface area, the more influential is in promoting complete combustion (Bakar et al., 2024).

Furthermore,  $\text{Al}_2\text{O}_3$  nanoparticles are reactive due to their high surface-to-volume ratio. The increased reactivity allows fuel molecules to be broken down and oxidized, reducing HC emissions. Nanoparticles of  $\text{Al}_2\text{O}_3$  are capable of storing and releasing oxygen during combustion. As a result, oxygen is kept available for oxidation reactions even in fuel-rich areas. It is possible to release oxygen stored during combustion, promoting more complete combustion and reducing HC emissions (Algayyim et al., 2024).  $\text{Al}_2\text{O}_3$  nanoparticles can also improve combustion chamber fuel-air mixing.

### Smoke emissions

Smoke emissions from diesel engines are a significant concern because of their adverse health and environmental effects; as a result, air pollution, respiratory problems, and

climate change occur. As a result, reducing smoke emissions from diesel engines has become an increasingly important research focus.

Figure 8 illustrates smoke for various fuel blends, combustion modes, and the presence or absence of  $\text{Al}_2\text{O}_3$  nano additive. For all fuels tested in DI mode without nano additive, smoke emissions increased with increasing load. With a Filter Smoke Number (FSN) value of 4.40, diesel (D) produced the highest smoke emissions at maximum load. A reduction in smoke emissions was observed after neem oil biodiesel was added to diesel. B25D75, B50D50, B75D25, and pure biodiesel showed FSN values of 3.98, 3.64, 3.49, and 3.40, respectively, at maximum load. Biodiesel is enriched with oxygen, promoting better combustion and reducing soot particles and smoke emissions. In comparing diesel and pure biodiesel at maximum load, biodiesel reduced smoke emissions by 22.7%.

Compared to diesel at maximum load, B25D75, B50D50, and B75D25, they reduced smoke emissions by 9.5%, 17.3%, and 20.7%, respectively. Biodiesel is estimated to contain 10-12% oxygen by weight, while diesel fuel contains minimal or no oxygen. By oxidizing soot particles during combustion, biodiesel produces better results. Enhancing oxidation breaks down soot particles, resulting in lower smoke emissions. This is because oxygen molecules react with the carbon atoms in the fuel, producing a more complete combustion (Dubey et al., 2022).

Biodiesel has a lower carbon content, and the hydrogen-to-carbon ratio is higher than that of diesel fuel. As biodiesel contains less carbon, soot particles are less likely to form during combustion. In addition, biodiesel forms more water vapour during combustion because of its high hydrogen-to-carbon ratio. This helps to reduce soot production. As a result of the combined effects of lower carbon content and a higher hydrogen-to-carbon ratio in biodiesel, smoke emissions are reduced (Ağbulut et al., 2019).

It is known that diesel fuel contains aromatic compounds, which contribute to the formation of soot during combustion. Soot particles are formed due to polycyclic aromatic hydrocarbons (PAH), a precursor to aromatic compounds. Biodiesel is virtually aromatic compound-free. Due to their absence in biodiesel, these compounds do not contribute to forming PAHs, thereby reducing soot formation. Compared with diesel fuel, biodiesel blends significantly reduce smoke emissions (Luo et al., 2022). In biodiesel, more oxygen content, reduced carbon content, a higher hydrogen-to-carbon ratio, and lack of aromatic compounds all contribute to complete combustion and significantly lower smoke emissions when using biodiesel blends.

Diesel and neem oil biodiesel blends in HCCI-DI mode without nano additives exhibit similar smoke emission characteristics to those observed in DI mode. HCCI-DI mode, however, emitted significantly fewer smoke particles than the DI mode for all fuels tested. As a result of the HCCI-DI mode, diesel (DEE-D) produced the most smoke emissions, with an FSN of 2.68 at maximum load. A reduction in smoke emissions was observed when neem oil biodiesel was added to diesel in HCCI-DI mode. In maximum load situations, DEE-B25D75, DEE-B50D50, DEE-B75D25, and pure biodiesel (DEE-B) all exhibited FSN values of 2.61, 2.60, 2.57, and 2.59, respectively. A comparison of diesel and biodiesel in HCCI-DI mode at

maximum load indicated that biodiesel decreased smoke emissions by 3.4%.

Significant differences were observed between diesel and pure neem oil biodiesel when they were compared in DI and HCCI-DI modes without nano additives. In DI mode, diesel produced the highest smoke emissions, with an FSN of 4.40 at maximum load. With HCCI-DI mode (DEE-D), diesel smoke emissions were significantly reduced, with an FSN of 2.68 at maximum load. HCCI-DI mode reduces diesel smoke emissions by 39.1% compared to DI mode. In HCCI-DI mode, pure neem oil biodiesel minimizes smoke emissions by 23.8% over diesel.

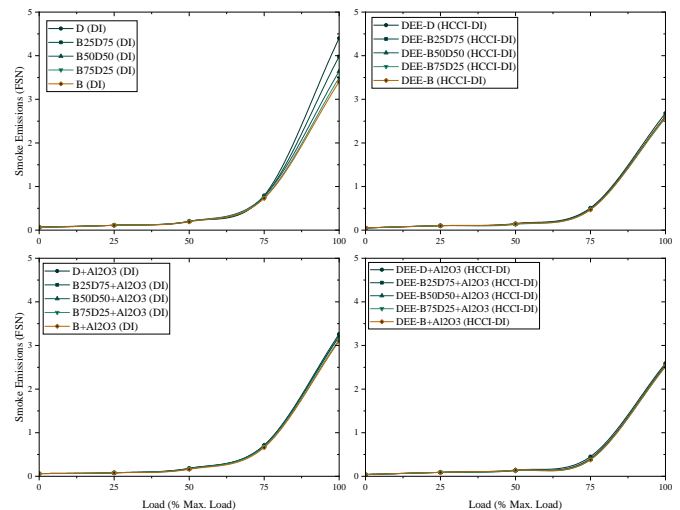


**Figure 8.** Variations of smoke emissions for different fuel blends, combustion modes, and  $\text{Al}_2\text{O}_3$  nano additive

As a result of fundamental differences between HCCI-DI and DI, HCCI-DI emits lower smoke emissions than DI for diesel and pure biodiesel. When fuel is injected into the chamber, a heterogeneous mixture of fuel and air is produced during the compression stroke. Consequently, local fuel-rich regions are prone to soot formation and higher smoke emissions. HCCI-DI, on the other hand, uses a dual-fuel approach to create a homogeneous mixture with air by injecting some fuel during the intake stroke. By premixing the combustion fuel, the HCCI-DI mode produces more complete and cleaner combustion, resulting in fewer local fuel-rich regions and lower smoke emissions than the DI mode (Hosseini et al., 2023).

When  $\text{Al}_2\text{O}_3$  nano additive is added to diesel ( $\text{D}+\text{Al}_2\text{O}_3$ ), smoke emissions decrease significantly. The FSN value of  $\text{D}+\text{Al}_2\text{O}_3$  at maximum load was 3.26, representing a reduction in smoke emissions of 25.9% over diesel. Smoke emissions were reduced when pure neem oil biodiesel ( $\text{B}+\text{Al}_2\text{O}_3$ ) was added with  $\text{Al}_2\text{O}_3$  nano additive in DI mode. Compared to neat biodiesel,  $\text{B}+\text{Al}_2\text{O}_3$  showed an FSN value of 3.10 at maximum load, which is an 8.8% reduction in smoke emissions. HCCI-DI mode also produced significant smoke emissions when  $\text{Al}_2\text{O}_3$  nano additives were added. With  $\text{Al}_2\text{O}_3$  nano additives added to diesel, the FSN value was 2.59 at maximum load, representing a 3.4% reduction in smoke emissions compared to DEE-D.  $\text{Al}_2\text{O}_3$  nano additives added to pure neem oil biodiesel ( $\text{DEE-B}+\text{Al}_2\text{O}_3$ ) resulted in a 2.7% reduction in smoke emissions over DEE-B at maximum load.

An  $\text{Al}_2\text{O}_3$  nanoparticle has an excellent surface-to-volume ratio and excellent catalytic properties. As catalysts, these

nanoparticles facilitate the complete oxidation of soot particles, which reduces smoke emissions during combustion. As a result of  $\text{Al}_2\text{O}_3$  nanoparticles' catalytic action, soot precursors, such as PAHs, are oxidized more rapidly, and soot is inhibited from forming. The presence of  $\text{Al}_2\text{O}_3$  nanoparticles improves fuel atomization and mixing processes. As a result of the reduction in nanoparticle size and increased surface area, fuel spray characteristics are improved. Fuel-air mixtures are more homogeneous due to improved atomization and mixing, which reduces smoke emissions and promotes cleaner combustion (Hariharan et al., 2021). Due to  $\text{Al}_2\text{O}_3$  nanoparticles' high thermal conductivity, the combustion chamber can transfer heat more efficiently. Through improved heat transfer, soot particles are reduced, lowering smoke emissions.

## CO emissions

The study of CO emissions in CI engines has gained significant attention in the quest for cleaner and more efficient combustion. The detrimental impact of CO emissions on air quality and human health makes them a considerable concern. The incomplete combustion of hydrocarbon fuels primarily causes CO emissions from CI engines. Figure 9 shows the CO emissions from different fuel blends, combustion modes, and the presence or absence of  $\text{Al}_2\text{O}_3$  nano additive.

Experimentally, diesel fuel emits more CO than biodiesel blends. Biodiesel, B25D75, B50D50, and B75D25 emit 0.08%, 0.07%, 0.06%, and 0.05% CO at 100% load. When biodiesel is added to fuel blends, CO emissions are significantly reduced. Having an inherent oxygen content, biodiesel enhances combustion, reducing carbon monoxide formation. During combustion, biodiesel oxygen facilitates CO oxidation into  $\text{CO}_2$ . As a result of biodiesel's higher cetane rating, it has a shorter ignition delay and better combustion quality than diesel (Hariharan et al., 2021). The combustion chamber will be less likely to have fuel-rich regions, which are more likely to produce CO. DEE-D emits 0.07% CO at 100% load, while DEE-B25D75, DEE-B50D50, DEE-B75D25, and pure biodiesel (DEE-B) emit 0.06%, 0.06%, 0.05%, and 0.04% CO. The trend indicates that increasing biodiesel content also reduces CO emissions during HCCI-DI.

The HCCI-DI mode shows lower CO emissions than the DI mode. 0.09% CO is emitted by diesel fuel when used in DI mode, whereas 0.05% CO is emitted by biodiesel. The HCCI-DI mode emits 0.07% CO for diesel (DEE-D) and 0.04% for biodiesel (DEE-B). HCCI-DI's improved combustion characteristics and homogeneous charge CI process are responsible for this significant reduction in CO emissions. When HCCI-DI is used, a portion of the fuel is injected at intake to promote a more uniform mixture. A more complete and efficient combustion process results from the CI of this homogeneous mixture. With HCCI mode, localized fuel-rich regions producing CO are less likely to occur as fuel and air mix better (Li et al., 2023).

In DI and HCCI-DI modes,  $\text{Al}_2\text{O}_3$  nanoparticles reduce CO compared to neat fuel. The CO emission rate of D+ $\text{Al}_2\text{O}_3$  is 0.04% at 100% load, while the CO emission rate of D is 0.09%.  $\text{Al}_2\text{O}_3$  nanoparticles play a catalytic role in this reduction by enhancing fuel oxidation, resulting in more complete combustion. In addition, nanoparticles improve fuel

atomization and mixing, improving the combustion process and producing less CO. DEE-D+ $\text{Al}_2\text{O}_3$  emits 0.03% CO at maximum load, while DEE-D emits 0.07%. The combination of HCCI combustion and nano additives in diesel fuel minimizes CO significantly. In combination with the nanoparticles' catalytic action and the improved mixing induced by the premixed fuel, such a combustion results in a more complete and efficient combustion. This results in a reduction in CO production [51].

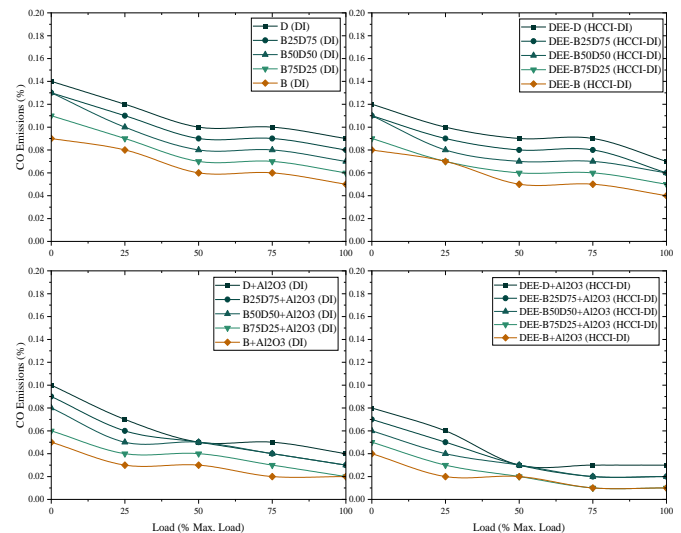


**Figure 9.** Variations of CO emissions for different fuel blends, combustion modes, and  $\text{Al}_2\text{O}_3$  nano additive

## CONCLUSION

The HCCI-DI engine was studied with and without nano  $\text{Al}_2\text{O}_3$  additives, fuelled with neem oil biodiesel and diesel. These findings provide valuable insight into the potential benefits of using biodiesel blends, HCCI-DI combustion mode, and nano additives in CI engines.

- The peak pressures of pure diesel in DI and HCCI-DI modes were higher than those of pure biodiesel by 2.17% and 1.23%, respectively. In DI and HCCI-DI modes,  $\text{Al}_2\text{O}_3$  nano additive increased peak pressures by 2.34% and 1.52% for diesel, and 3.23% and 0.52% for biodiesel, respectively.
- The HRR<sub>max</sub> decreased by 19.63% when biodiesel content was increased from 0% to 100% in DI mode. Diesel and biodiesel HRR<sub>max</sub> were higher in the HCCI-DI than in the DI by 9.27% and 28.26%, respectively. HRR<sub>max</sub> for diesel in DI and HCCI-DI modes was enhanced by 3.09% and 1.63%, respectively, by adding an  $\text{Al}_2\text{O}_3$  nano additive.
- Compared to diesel, biodiesel reduces BTE by 2.01% when run in DI mode and 1.68% when run in HCCI-DI. In HCCI-DI, BTE was improved by 0.18% for diesel and 0.51% for biodiesel. Diesel and biodiesel BTE increased by 0.85% and 0.1%, respectively, when the nano  $\text{Al}_2\text{O}_3$  was added in DI mode and by 0.34% and 0.01% when the nano  $\text{Al}_2\text{O}_3$  was added in HCCI-DI mode.
- HCCI-DI modes reduced NO<sub>x</sub> emissions by 4.3% and 10.9% for diesel and biodiesel, respectively.
- Biodiesel in DI mode reduced HC emissions by 52.17%. HC emissions were reduced by 13.04-18.18% in DI mode and 18.75-19.51% in HCCI-DI mode by adding the  $\text{Al}_2\text{O}_3$  nano additive.
- Smoke emissions decreased by 22.7% in DI mode with biodiesel and 23.8-39.1% in HCCI-DI mode. The addition of an  $\text{Al}_2\text{O}_3$  nano additive further reduced smoke emissions.

- Biodiesel reduced CO emissions by 42.86-44.44% in both modes. With the Al<sub>2</sub>O<sub>3</sub> nano additive, diesel CO emissions dropped 55.56%, and biodiesel emissions fell 20%.

Future research could explore several avenues to build on these findings. First, investigating the effects of varying nanoparticle concentrations (beyond 50 ppm) and different nanoparticle types (e.g., CeO<sub>2</sub>, TiO<sub>2</sub>) could optimize combustion efficiency and emission reductions further. Second, a detailed study on the long-term durability of engine components under HCCI-DI operation with biodiesel-nanoparticle blends would address practical implementation concerns. Third, integrating advanced combustion control strategies, such as variable injection timing or exhaust gas recirculation (EGR), could enhance the balance between thermal efficiency and NO<sub>x</sub> emissions. Finally, a lifecycle assessment of neem oil biodiesel production and nanoparticle synthesis would provide insights into the environmental sustainability of this approach, broadening its applicability in real-world scenarios.

## REFERENCES

Ağbulut, Ü., Sarıdemir, S., & Albayrak, S. (2019). Experimental investigation of combustion, performance and emission characteristics of a diesel engine fuelled with diesel-biodiesel-alcohol blends. *Journal of the Brazilian Society of Mechanical Sciences and Engineering*, 41(9). <https://doi.org/10.1007/S40430-019-1891-8>

Al-Dawody, M. F., Al-Farhany, K. A., Hamza, N. H., & Hamzah, D. A. (2021a). Numerical study for the spray characteristics of a diesel engine powered by biodiesel fuels under different injection pressures. *Journal of Engineering Research*. <https://doi.org/10.36909/jer.9821>

Algayyim, S. J. M., Saleh, K., Wandel, A. P., Fattah, I. M. R., Yusaf, T., & Alrazen, H. A. (2024). Influence of natural gas and hydrogen properties on internal combustion engine performance, combustion, and emissions: A review. *Fuel*, 362. <https://doi.org/10.1016/J.FUEL.2023.130844>

Bakar, R. A., Widudo, Kadirgama, K., Ramasamy, D., Yusaf, T., Kamarulzaman, M. K., Sivaraos, Aslfattahi, N., Samyilingam, L., & Alwayzy, S. H. (2024). Experimental analysis on the performance, combustion/emission characteristics of a DI diesel engine using hydrogen in dual fuel mode. *International Journal of Hydrogen Energy*, 52, 843–860. <https://doi.org/10.1016/J.IJHYDENE.2022.04.129>

Bazdidi-Tehrani, F., Sharifi-Sedeh, E., & Abedinejad, M. S. (2023). Effects of alumina nanoparticles on evaporation and combustion characteristics of diesel fuel droplets. *Journal of the Taiwan Institute of Chemical Engineers*, 143, 104713. <https://doi.org/10.1016/j.jtice.2023.104713>

Beyaz, M., Aydın, S., & Şener, R. (2025). Influence of ethyl proxitol on cold filter plugging point, combustion, emissions characteristics of biodiesel blends in CI engines. *Petroleum Science and Technology*, 43(3), 284–304. <https://doi.org/10.1080/10916466.2023.2292783>

Bhikuning, A., Irhashi, Z. R., & Aldebaran, D. (2022). The Simulation of Combustion Characteristics from Diesel Fuel and Biodiesel in Different Engine Rotation. *Aceh*

*International Journal of Science and Technology*, 11(3), 182–189. <https://doi.org/10.13170/aijst.11.3.22711>

Chen, G., Kong, W., Xu, Y., Shen, Y., & Wei, F. (2024). Thermal efficiency and emissions improvement of the lean burn high compression ratio HPDI NG engine at different combustion modes. *Applied Thermal Engineering*, 247, 123061. <https://doi.org/10.1016/J.APPLTHERMALENG.2024.123061>

Coskun, G., Soyhan, H. S., Demir, U., Turkcan, A., Ozsezen, A. N., & Canakci, M. (2014). Influences of second injection variations on combustion and emissions of an HCCI-DI engine: Experiments and CFD modelling. *Fuel*, 136, 287–294. <https://doi.org/10.1016/j.fuel.2014.07.042>

Da Silva Medeiros, D. C. C., Usman, M., Chelme-Ayala, P., & Gamal El-Din, M. (2025). Biochar-enhanced removal of naphthenic acids from oil sands process water: Influence of feedstock and chemical activation. *Energy & Environmental Sustainability*, 1(2), 100028. doi: <https://doi.org/10.1016/j.eesus.2025.100028>

Dash, S. K., Elumalai, P. V., Ranjit, P. S., Das, P. K., Kumar, R., Kunar, S., & Papu, N. H. (2021). Experimental investigation on synthesis of biodiesel from non-edible Neem seed oil: Production optimization and evaluation of fuel properties. *Materials Today: Proceedings*, 47, 2463–2466. <https://doi.org/10.1016/j.matpr.2021.04.551>

Dhahad, H. A., Ali, S. A., & Chaichan, M. T. (2020). Combustion analysis and performance characteristics of compression ignition engines with diesel fuel supplemented with nano-TiO<sub>2</sub> and nano-Al<sub>2</sub>O<sub>3</sub>. *Case Studies in Thermal Engineering*, 20, 100651. <https://doi.org/10.1016/j.csite.2020.100651>

Dubey, A., Prasad, R. S., Singh, J. K., & Nayyar, A. (2022). Combined effects of biodiesel – ULSD blends and EGR on performance and emissions of diesel engine using Response surface methodology (RSM). *Energy Nexus*, 7, 100136. <https://doi.org/10.1016/J.NEXUS.2022.100136>

Fang, J., Wang, K., Chen, P., Xu, X., Zhang, C., Wu, Y.,... Zuo, Z. (2025). Oxidation of Soot by Cerium Dioxide Synthesized Under Different Hydrothermal Conditions. *Molecules*, 30(5), 1161. <https://doi.org/10.3390/molecules30051161>

Farokhi, G., Saidi, M., & Najafabadi, A. T. (2023). Application of spinel Type Ni<sub>x</sub>Zn<sub>1-x</sub>Fe<sub>2</sub>O<sub>4</sub> magnetic nanocatalysts for biodiesel production from neem seed oil: Catalytic performance evaluation and optimization. *Industrial Crops and Products*, 192, 116035. <https://doi.org/10.1016/j.indcrop.2022.116035>

G M, L. L., M, C. Das, Jayabal, R., S, M., D, S., & N, M. (2023). Experimental evaluation and neural network modelling of reactivity-controlled compression ignition engine using cashew nut shell oil biodiesel-alumina nanoparticle blend and gasoline injection. *Energy*, 282, 128923. <https://doi.org/10.1016/j.energy.2023.128923>

Hariharan, D., Rajan Krishnan, S., Kumar Srinivasan, K., & Sohail, A. (2021). Multiple injection strategies for reducing HC and CO emissions in diesel-methane dual-fuel low temperature combustion. *Fuel*, 305, 121372. <https://doi.org/10.1016/J.FUEL.2021.121372>

- Hosseini, S. H., Tsolakis, A., Alagumalai, A., Mahian, O., Lam, S. S., Pan, J., Peng, W., Tabatabaei, M., & Aghbashlo, M. (2023). Use of hydrogen in dual-fuel diesel engines. *Progress in Energy and Combustion Science*, 98, 101100. <https://doi.org/10.1016/j.pecs.2023.101100>
- Jairam, K., Mohammed Musthafa, F., Annanth Vijayan, K., & Renganathan, M. (2021). Computational investigations on port injected DEE in a biogas inducted HCCI engine. *International Journal for Simulation and Multidisciplinary Design Optimization*, 12, 9. <https://doi.org/10.1051/smdo/2021010>
- Jayabal R. (2024). Optimization and impact of modified operating parameters of a diesel engine emissions characteristic utilizing waste fat biodiesel/di-tert-butyl peroxide blend. *Process Safety and Environmental Protection*, 186, 694-705. <https://doi.org/j.psep.2024.04.019>
- Jayabal R. (2025). Environmental impact of adding hybrid nanoparticles and hydrogen to the algae biodiesel-diesel blend on engine emissions. *Process Safety and Environmental Protection*, 198, <https://doi.org/j.psep.2025.107102>
- Jokubynienė, V., Slavinskas, S., & Kreivaitis, R. (2023). The Effect of Nanoparticle Additives on the Lubricity of Diesel and Biodiesel Fuels. *Lubricants*, 11(7), 290. <https://doi.org/10.3390/lubricants11070290>
- Leo, G. M. L., Sekar, S., & Arivazhagan, S. (2020). Experimental investigation and ANN modelling of the effects of diesel/gasoline premixing in a waste cooking oil-fuelled HCCI-DI engine. *Journal of Thermal Analysis and Calorimetry*, 141(6), 2311-2324. <https://doi.org/10.1007/S10973-020-09418-Z>
- Leo, G. M. L., Thodda, G., & Murugapoopathi, S. (2021). Experimental investigation on effects of gasoline premixed - Al<sub>2</sub>O<sub>3</sub> additive blended fish oil biodiesel fuelled HCCI-DI engine. *Journal of Physics: Conference Series*, 2054(1), 012040. <https://doi.org/10.1088/1742-6596/2054/1/012040>
- Li, Z., Liu, J., Ji, Q., Sun, P., Wang, X., & Xiang, P. (2023). Influence of hydrogen fraction and injection timing on in-cylinder combustion and emission characteristics of hydrogen-diesel dual-fuel engine. *Fuel Processing Technology*, 252, 107990. <https://doi.org/10.1016/j.fuproc.2023.107990>
- Liao, H., Hu, F., Wu, X., Li, P., Ding, C., Yang, C., Zhang, T., & Liu, Z. (2024). Effects of H<sub>2</sub> addition on the characteristics of the reaction zone and NO<sub>x</sub> mechanisms in MILD combustion of H<sub>2</sub>-rich fuels. *International Journal of Hydrogen Energy*, 58, 174-189. <https://doi.org/10.1016/j.ijhydene.2024.01.154>
- Lionus Leo G.M., Jayabal R., Srinivasan, D., Chrispin Das, M., Ganesh, M., & Gavaskar, T. (2024). Predicting the performance and emissions of an HCCI-DI engine powered by waste cooking oil biodiesel with Al<sub>2</sub>O<sub>3</sub> and FeCl<sub>3</sub> nano additives and gasoline injection – A random forest machine learning approach. *Fuel*, 357. <https://doi.org/10.1016/j.fuel.2023.129914>
- Lionus Leo, G. M., Murugapoopathi, S., Thodda, G., Baligheid, S. M., Jayabal, R., Nedunchezhiyan, M., & Devarajan, Y. (2023). Optimisation and environmental analysis of waste cashew nut shell oil biodiesel/cerium oxide nanoparticles blends and acetylene fumigation in agricultural diesel engine. *Sustainable Energy Technologies and Assessments*, 58, 103375. <https://doi.org/10.1016/j.seta.2023.103375>
- Lionus Leo G.M., Jayabal R., Kathapillai A., Sekar S. (2025a). Performance and emissions optimization of a dual-fuel diesel engine powered by cashew nut shell oil biodiesel/hydrogen gas using response surface methodology. *Fuel*, 384, <https://doi.org/j.fuel.2024.133960>
- Lionus Leo G.M., Jayabal R., Chrispin Das M., Arivazhagan S. (2025b). An experimental investigation on enhancing diesel engine performance and emissions with cashew nut shell oil biodiesel and hydrogen fumigation. *Environment, Development and Sustainability*. <https://doi.org/s10668-024-05565-7>
- Luo, J., Liu, Z., Wang, J., Xu, H., Tie, Y., Yang, D., Zhang, Z., Zhang, C., & Wang, H. (2022). Investigation of hydrogen addition on the combustion, performance, and emission characteristics of a heavy-duty engine fueled with diesel/natural gas. *Energy*, 260, 125082. <https://doi.org/10.1016/j.energy.2022.125082>
- Madihi, R., Pourfallah, M., Gholinia, M., Armin, M., & Ghadi, A. Z. (2022). Thermofluids analysis of combustion, emissions, and energy in a biodiesel (C<sub>11</sub>H<sub>22</sub>O<sub>2</sub>) / natural gas heavy-duty engine with RCCI mode (Part II: Fuel injection time/ Fuel injection rate). *International Journal of Thermofluids*, 16, 100200. <https://doi.org/10.1016/j.ijft.2022.100200>
- Mary, L. L. G., Manivel, S., Garg, S., Nagam, V. B., Garse, K., Mali, R., Yunus Khan, T. M., & Baig, R. U. (2023). Exploring the Impact of Al<sub>2</sub>O<sub>3</sub> Additives in Gasoline on HCCI-DI Engine Performance: An Experimental, Neural Network, and Regression Analysis Approach. *ACS Omega*, 8(50), 47701-47713. <https://doi.org/10.1021/ACSOMEGA.3C05959>
- Mathiyazhagan, M., Meenakshi Sundaram, K., & Bupesh, G. (2022). Production and emission evaluation of neem biodiesel blends in a single cylinder diesel engine. *Materials Today: Proceedings*, 62, 2124-2132. <https://doi.org/10.1016/j.matpr.2022.03.047>
- Mishra, A., Kulshrestha, S., Patel, F. M., Tiwari, N., & Sharma, A. (2024). Effect of piston bowl geometry and spray angle on engine performance and emissions in HCCI engine using multi-stage injection strategy. *Environmental Progress & Sustainable Energy*, 43(2). <https://doi.org/10.1002/ep.14203>
- Mohankumar, D., Indharajith, P., Sabarishankar, P., Sanjaykumar, V. T., Vignesh kumar, N., & Udhayakumar, N. (2023). Experimental investigation on performance, emission and combustion characteristics of neem oil bio diesel using ethanol blend. *Materials Today: Proceedings*, 80, 1525-1529. <https://doi.org/10.1016/j.matpr.2023.01.352>
- Mohanrajhu N., Sekar S., Jayabal R., Sureshkumar R. (2024). Impact of Aluminum Nitrate and Graphene Oxide Nanoplate on Performance and Emission Characteristics of a CRDI Diesel Engine Powered by Industrial Leather Waste Fat Biodiesel. *International Journal of Automotive Technology*, <https://doi.org/s12239-024-00205-5>

- Vellaiyan, S. (2025a). Optimization of hydrogen-enriched biodiesel-diesel dual-fuel combustion with EGR for sustainable engine performance. *International Journal of Hydrogen Energy*, 128, 85–94. <https://doi.org/10.1016/j.ijhydene.2025.04.239>
- Vellaiyan, S. (2025b). Performance enhancement of a diesel engine using nanoparticle-enriched algae biodiesel-diesel blends with an electrostatic precipitator for nanoparticle emission control. *Energy Conversion and Management*, 326, 119457. <https://doi.org/10.1016/j.enconman.2024.119457>
- Savaş, A., Uslu, S., & Şener, R. (2025). Optimization of performance and emission characteristics of a diesel engine fueled with MgCO<sub>3</sub> nanoparticle doped second generation biodiesel from jojoba by using response surface methodology (RSM). *Fuel*, 381, 133658. <https://doi.org/10.1016/j.fuel.2024.133658>
- Sekar, S., Chandrasekar, P., Kumar, S., Jospher, A. J. S., Sheeja, R., Valarmathi, T. N., & Lionus Leo, G. M. (2021). Entropy Generation Minimization of Vapour Absorption Heat Transformer. *Lecture Notes in Mechanical Engineering*, 265–274. [https://doi.org/10.1007/978-981-33-4165-4\\_25](https://doi.org/10.1007/978-981-33-4165-4_25)
- ŞENER, R. (2021). Experimental and Numerical Analysis of a Waste Cooking Oil Biodiesel Blend used in a CI Engine. *International Journal of Advances in Engineering and Pure Sciences*, 33(2), 299–307. <https://doi.org/10.7240/ieps.829006>
- Sheik, M. A., Beemkumar, N., Gupta, A., Gill, A., Devarajan, Y., Jayabal, R., & Lionus Leo, G. M. (2024). Study the Effect of Silicon Nanofluid on the Heat Transfer Enhancement of Triangular-Shaped Open Microchannel Heat Sinks. *Silicon*, 16(1), 277–293. <https://doi.org/10.1007/S12633-023-02663-5>
- Shivkumar, C., Amar, P., & Mitesh, G. (2021). Experimental Investigation on VCR Engine by Using Different Blend Proportions of Mexicana Oil Biodiesel. In *Techno-Societal 2020* (pp. 437–443). Springer International Publishing. [https://doi.org/10.1007/978-3-030-69925-3\\_43](https://doi.org/10.1007/978-3-030-69925-3_43)
- Simhadri, K., Rao, P. S., & Paswan, M. (2024). Improving the combustion and emission performance of a diesel engine with TiO<sub>2</sub> nanoparticle blended Mahua biodiesel at different injection pressures. *International Journal of Thermofluids*, 21, 100563. <https://doi.org/10.1016/j.ijft.2024.100563>
- SivaPrasad, K., Rao, S. S., & Raju, V. R. K. (2022). Enhancement of mixture homogeneity for DI-CI engine to achieve Homogeneous Charge Compression Ignition (HCCI) combustion characteristics: a numerical approach. *Energy Sources, Part A: Recovery, Utilization, and Environmental Effects*, 44(2), 4318–4333. <https://doi.org/10.1080/15567036.2022.2075058>
- Spanò, S., Savarese, M., Parente, A., Contino, F., & Jeanmart, H. (2024). Experimental and numerical investigation of methane combustion in a HCCI engine under enriched oxygen conditions. *Fuel*, 362, 130772. <https://doi.org/10.1016/j.fuel.2023.130772>
- Subramani, S., Dana, S. S., Natesan, V. T., & Mary, L. L. G. (2020). Energy and exergy analysis of greenhouse drying of ivy gourd and turkey berry. *Thermal Science*, 24(1 Part B), 645–656. <https://doi.org/10.2298/TSCI190602459S>
- Tai, M., Vo, C., Duong, L., Do, A., Huynh, V., & Nguyen, H. (2023). Experimental Study on Combustion Characteristics of Biodiesel–Ethanol Dual Fuel: An Overview. *Journal of Technical Education Science*, 75A, 50–60. <https://doi.org/10.54644/jte.75A.2023.1269>
- Varpe, B. R., & Kharde, Y. R. (2023). Combined effect of DEE and Jatropha biodiesel–diesel fuel blends on the enhancement of VCR diesel engine parameters at varying loads and compression ratios. *Australian Journal of Mechanical Engineering*, 21(5), 1843–1860. <https://doi.org/10.1080/14484846.2022.2038405>
- Venkatesan, S. P., & Kadiresh, P. N. (2015). Effects of Nano-Sized Metal Oxide Additive on Performance and Exhaust Emissions of C I Engine. *Applied Mechanics and Materials*, 766–767, 389–395. <https://doi.org/10.4028/www.scientific.net/AMM.766-767.389>
- Veza, I., Irianto, Tuan Hoang, A., Yusuf, A. A., Herawan, S. G., Soudagar, M. E. M., Samuel, O. D., Said, M. F. M., & Silitonga, A. S. (2023). Effects of Acetone-Butanol-Ethanol (ABE) addition on HCCI-DI engine performance, combustion and emission. *Fuel*, 333, 126377. <https://doi.org/10.1016/j.fuel.2022.126377>
- Yasar, F., Uguz, G., & Kayunoglu, C. (2022). Change in Calculated Carbon Aromaticity Index (CCAI) Depending on Cetane Indexes of Biodiesel Fuels of Different Origins. *2022 Global Energy Conference (GEC)*, 352–356. <https://doi.org/10.1109/GEC55014.2022.9986785>
- Zhang, L., Zhu, G., Chao, Y., Chen, L., & Ghanbari, A. (2023). Simultaneous prediction of CO<sub>2</sub>, CO, and NO<sub>x</sub> emissions of biodiesel-hydrogen blend combustion in compression ignition engines by supervised machine learning tools. *Energy*, 282, 128972. <https://doi.org/10.1016/J.ENERGY.2023.128972>
- Zhang, S., Li, J., Tian, Y., Fang, S., Li, C., Yu, X.,... Yang, L. (2025). Probing the combustion characteristics of micron-sized aluminum particles enhanced with graphene fluoride. *Combustion and Flame*, 272, 113858. <https://doi.org/10.1016/j.combustflame.2024.113858>
- Zhang, W., Shi, L., Xia, W., Du, Y., & Yao, L. (2025). Research on the anharmonic effect of main reactions of important intermediate species in NH<sub>3</sub>/DME mixed combustion. *Chemical Physics Letters*, 874–875, 142170. <https://doi.org/10.1016/j.cplett.2025.142170>
- Zhang, Y., Zhong, Y., Wang, J., Tan, D., Zhang, Z., & Yang, D. (2021). Effects of Different Biodiesel-Diesel Blend Fuel on Combustion and Emission Characteristics of a Diesel Engine. *Processes*, 9(11), 2021. <https://doi.org/10.3390/pr9111984>
- Zhu, L., Song, Y., Chen, H., Wang, M., Liu, Z., Wei, X.,... Ai, T. (2025). Optimization of power generation and sewage treatment in stacked pulsating gas-liquid-solid circulating fluidized bed microbial fuel cell using response surface methodology. *International Journal of Hydrogen Energy*, 101, 161–172. <https://doi.org/10.1016/j.ijhydene.2024.12.397>